



Short communication

## Fabrication of hollow-structured FeO<sub>x</sub>-MnO<sub>x</sub> oxidative catalysts with ultra-large surface area



Baohuai Zhao<sup>a</sup>, Zesheng Yang<sup>a</sup>, Rui Ran<sup>a,\*</sup>, Zeliang Guo<sup>a</sup>, Xiaodong Wu<sup>b</sup>, Duan Weng<sup>a,b,\*</sup>

<sup>a</sup> State Key Laboratory of New Ceramic and Fine Processing, School of Materials Science and Engineering, Tsinghua University, Beijing 100084, China

<sup>b</sup> Key Laboratory of Advanced Materials (MOE), School of Materials Science and Engineering, Tsinghua University, Beijing 100084, China

### ARTICLE INFO

#### Keywords:

MnO<sub>x</sub>  
Hollow structure  
Specific surface area  
Redox properties  
CO oxidation

### ABSTRACT

In this work, hollow-structured MnO<sub>x</sub> and FeO<sub>x</sub>-MnO<sub>x</sub> were synthesized by self-template route and applied for CO oxidation. FeO<sub>x</sub>-MnO<sub>x</sub> exhibited better catalytic activity than MnO<sub>x</sub>. It could convert 79.1% CO at 20 °C and had a higher CO conversion during the temperature ramping. The FeO<sub>x</sub> species could react with HCl and greatly helped to increase the specific surface area (428.5 m<sup>2</sup> g<sup>-1</sup>) and pore volume (0.82 cm<sup>3</sup> g<sup>-1</sup>) of the catalyst. The reserved FeO<sub>x</sub> in the FeO<sub>x</sub>-MnO<sub>x</sub> sample enhanced the redox properties and increased the amount of reactive oxygen species.

### 1. Introduction

MnO<sub>x</sub> has been extensively researched as an inexpensive and environmental-friendly material applied in catalytic oxidation of CO, NO, VOCs, etc. [1,2]. Given the fact that the morphologies and structure properties could significantly influence the catalytic performance of the material, remarkable progress has been made for the synthesis of MnO<sub>x</sub>. Various morphologies and phase structures were successfully obtained, including nanostructures (nano-tubes/-belts/-rods/-flakes, etc.) [3–6], ordered mesoporous structures [7], and some hierarchical structures (urchin-like/hollow sphere, etc.) [8–11].

Among the methods for preparing MnO<sub>x</sub> materials, acid treatment was a simple and effective way to create defects and porous structures [1,12,13]. Si et al. [13] selectively removed La<sup>3+</sup> cations from the LaMnO<sub>3+δ</sub> perovskite using diluted HNO<sub>3</sub> and obtained a γ-MnO<sub>2</sub>-like material. Such an oxide had a specific surface area of about 250 m<sup>2</sup> g<sup>-1</sup> and showed higher CO oxidation activity than the normal LaMnO<sub>3+δ</sub> and γ-MnO<sub>2</sub> synthesized by traditional methods. On the other hand, the self-template route using acid solution was a method to synthesize MnO<sub>x</sub> with hollow structures [14]. Dispersed MnCO<sub>3</sub> particles were firstly synthesized and an oxide shell was formed by the oxidation of carbonate using KMnO<sub>4</sub>. Then the carbonate core was selectively removed by acid solution. The as-prepared hollow MnO<sub>x</sub> was used in water treatment [15–17], supercapacitors [18], and Li-ion batteries [19,20]. The most attractive feature of the hollow MnO<sub>x</sub> prepared by such a self-template method was their high surface area. Cao et al. [17] calcined the samples at 400 °C for 4 h after acid leaching and got a kind of γ-MnO<sub>2</sub>/α-MnO<sub>2</sub> ellipsoids with a specific surface area of

~100 m<sup>2</sup> g<sup>-1</sup>. Yu and co-workers [18] obtained MnO<sub>2</sub> hollow structures without calcination and the samples had a specific surface area of about 300 m<sup>2</sup> g<sup>-1</sup>. However, few literature were focused on the behavior of manganese carbonate that mixed with other metal elements in the self-template route. A mixed oxide shell should be formed over the carbonate after the reaction with KMnO<sub>4</sub>. It is, therefore, possible that the specific surface area of the final oxide product would be further increased if some less acid-stable metal oxide such as FeO<sub>x</sub> and CoO<sub>x</sub> are chosen. And the physicochemical properties of the base material MnO<sub>x</sub> may also be tuned.

In the present study, we fabricated hollow MnO<sub>x</sub> and FeO<sub>x</sub>-MnO<sub>x</sub> structures with large specific surface areas and evaluated their catalytic performance for CO oxidation. With Fe doping into the carbonate precursor, the specific surface area and pore volume of the final FeO<sub>x</sub>-MnO<sub>x</sub> product were remarkably increased. The physicochemical properties of the catalysts were also studied.

### 2. Experimental

#### 2.1. Synthesis of MnO<sub>x</sub> and FeO<sub>x</sub>-MnO<sub>x</sub>

In this work, the hollow structures were synthesized in the way that was similar to the literature [15], and a scheme of the preparation was shown in Fig. S1. The MnCO<sub>3</sub> and Fe-doped carbonate (Mn/Fe = 4/1, denoted as Fe<sub>0.2</sub>Mn<sub>0.8</sub>CO<sub>3</sub>) were served as precursors and they were prepared using MnSO<sub>4</sub>·H<sub>2</sub>O (99%, Aladdin, China), FeSO<sub>4</sub>·7H<sub>2</sub>O (99%, Aladdin, China), and NaHCO<sub>3</sub> (99.8%, Aladdin, China). For the preparation of MnCO<sub>3</sub>, 0.01 mol MnSO<sub>4</sub>·H<sub>2</sub>O and 0.01 mol NaHCO<sub>3</sub> were

\* Corresponding author.

E-mail addresses: [ranr@tsinghua.edu.cn](mailto:ranr@tsinghua.edu.cn) (R. Ran), [duanweng@tsinghua.edu.cn](mailto:duanweng@tsinghua.edu.cn) (D. Weng).

separately dissolved in 700 mL deionized water. Then the  $\text{NaHCO}_3$  solution was added into the  $\text{MnSO}_4$  solution under stirring. The mixture was stirred for 12 h at room temperature. Finally, the suspension was filtered and washed with deionized water, followed by drying at  $80^\circ\text{C}$  in an oven overnight. For the preparation of  $\text{Fe}_{0.2}\text{Mn}_{0.8}\text{CO}_3$ , 0.008 mol  $\text{MnSO}_4\cdot\text{H}_2\text{O}$  and 0.002 mol  $\text{FeSO}_4\cdot 7\text{H}_2\text{O}$  were dissolved to form a homogeneous solution. The following steps were same to those of the preparation of  $\text{MnCO}_3$ .

For the preparation of  $\text{MnO}_x$  and  $\text{FeO}_x\text{-MnO}_x$ , 1 g of the as-prepared precursor of  $\text{MnCO}_3$  or  $\text{Fe}_{0.2}\text{Mn}_{0.8}\text{CO}_3$  was dispersed in 40 mL deionized water. Then 5 mL  $\text{KMnO}_4$  solution ( $0.032\text{ mol L}^{-1}$ ) was added under stirring. After being reacted for 40 min, 5 mL  $\text{HCl}$  solution ( $2.4\text{ mol L}^{-1}$ ) was added into the above solution, and the suspension was stirred for another 2 min. The precipitate was centrifuged and washed with deionized water and ethanol for several times and dried at  $110^\circ\text{C}$  overnight. Finally, the products were calcined in a muffle furnace at  $300^\circ\text{C}$  for 3 h in static air.

## 2.2. Catalyst characterization

The bulk compositions of the catalysts were measured by inductively coupled plasma atomic emission spectroscopy (ICP-AES). X-ray diffraction (XRD) was performed to determine the phase structures. The morphologies and sizes of the samples were observed using scanning electron microscopy (SEM) and transmission electron microscopy (TEM). The pore volume and specific surface area were determined by  $\text{N}_2$  adsorption/desorption experiments. The X-ray photoelectron spectroscopy (XPS) analysis was carried out to get the surface properties. The redox properties were measured by  $\text{H}_2$  temperature programmed reduction ( $\text{H}_2\text{-TPR}$ ). All of the characterizations mentioned above can be found in detail in our previous work [1,21,22].

## 2.3. CO catalytic oxidation tests

The CO catalytic oxidation activity was evaluated in a fixed-bed reactor with an inner diameter of 12 mm. 50 mg catalyst was put into the reactor and fixed by quartz wool on both ends. Before each test, the catalyst was pretreated at  $300^\circ\text{C}$  for 30 min in 10%  $\text{O}_2/\text{N}_2$  ( $100\text{ mL min}^{-1}$ ). Then the reactant gas mixture (5000 ppm CO, 10%  $\text{O}_2$ , balanced with  $\text{N}_2$ ) was introduced into the reactor system, with a total flow rate of  $100\text{ mL min}^{-1}$ , corresponding to a gas hourly space velocity (GHSV) of  $120,000\text{ mL g}_{\text{cat}}^{-1}\text{ h}^{-1}$ . The temperature was increased from 20 to  $250^\circ\text{C}$  with a heating rate of  $10^\circ\text{C min}^{-1}$ . The component concentrations in the effluent gas were detected by a Fourier-transform infrared spectrometer (Thermal Nicolet iS10) with a spectral resolution of  $0.5\text{ cm}^{-1}$ . The pretreatment and temperature ramping test were performed twice for each catalyst and the CO conversion was calculated according to  $(1 - [\text{CO}]_{\text{outlet}}/[\text{CO}]_{\text{inlet}}) \times 100\%$ .

## 3. Results and discussion

### 3.1. Phase structures and morphologies

The XRD patterns of the two carbonates in Fig. S2 show sharp characteristic peaks of rhombohedral  $\text{MnCO}_3$  phase (JCPDS No. 44–1472) without any impurities [18]. The diffraction peaks of  $\text{Fe}_{0.2}\text{Mn}_{0.8}\text{CO}_3$  slightly shift to higher angle positions; this indicates that the Fe ions are doping into the carbonate structure since the radius of  $\text{Fe}^{2+}$  ( $0.65\text{ \AA}$ ) is smaller than that of  $\text{Mn}^{2+}$  ( $0.83\text{ \AA}$ ) [23]. The XRD patterns shown in Fig. 1(a) correspond to the oxides derived from the carbonate precursors. They both match the pattern of the birnessite  $\text{MnO}_2$  (JCPDS No. 18–0802) [18,24,25]. The peaks centered at  $2\theta = 36.9^\circ$  and  $66.0^\circ$  could be well assigned to the (006) and (119) planes of  $\text{MnO}_2$ . However, the low intensities and broadening of the peaks reveal an amorphous or poorly ordered polycrystalline nature of the catalysts. For the XPS spectra of Mn 2p in Fig. 1(b), the two catalysts

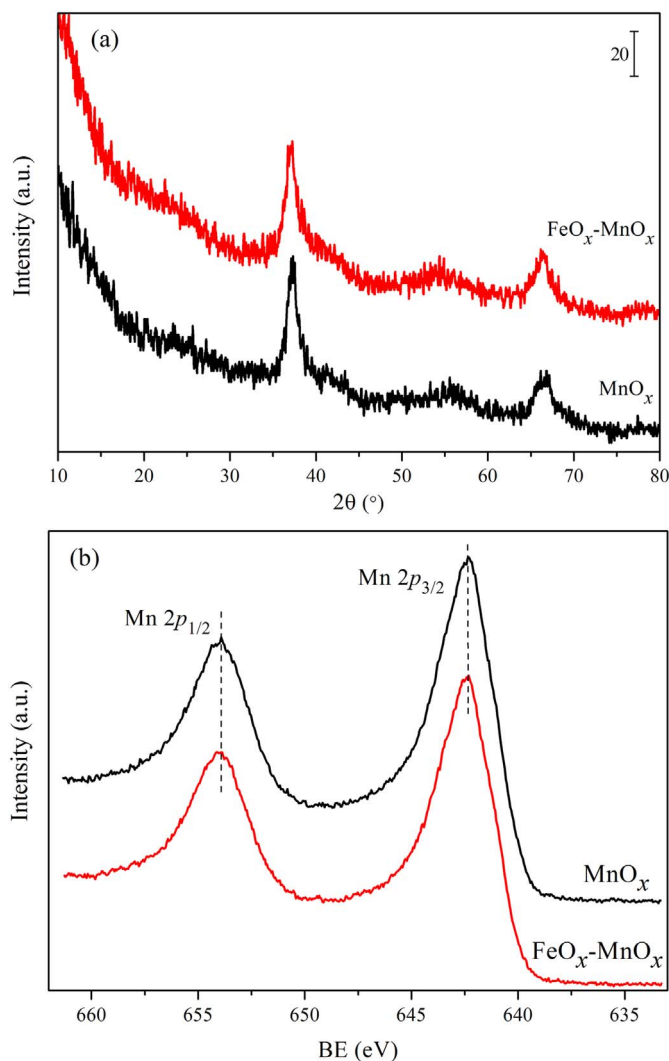


Fig. 1. (a) X-ray diffraction patterns and (b) Mn 2p XPS spectra of the catalysts.

have very similar spectra and two peaks centered at 653.9 and 642.3 eV can be found in each of the spectra, which are assigned to the  $\text{Mn } 2p_{1/2}$  and  $\text{Mn } 2p_{3/2}$ , respectively. That further proves the dominance of  $\text{MnO}_2$  in the catalysts [24,25].

Fig. 2 shows the SEM images of the oxides. As can be seen from their overall appearance in Fig. 2(a) and (b), the samples preserve the shapes and sizes of  $\text{MnCO}_3$  and  $\text{Fe}_{0.2}\text{Mn}_{0.8}\text{CO}_3$  precursors. The hollow structures of the  $\text{MnO}_x$  and  $\text{FeO}_x\text{-MnO}_x$  were created after the acid treatment. Some of the broken samples present the “shell-like” appearance, and the cavity inside the shell can be clearly seen in the magnified SEM images as insets in Fig. 2(a) and (b). The surface of the shells consists of a lot of curly sheets with a thickness in nanoscale. The formation of the oxide shells and nano-sheets proceeded simultaneously during the reaction between  $\text{KMnO}_4$  and carbonates [16]. For clearly explaining the formation of such a characterized morphology, more microscopic images are given in the “Supporting Information”. Fig. S3 presents the typical SEM images of the  $\text{MnCO}_3$  and  $\text{Fe}_{0.2}\text{Mn}_{0.8}\text{CO}_3$  particles. The  $\text{MnCO}_3$  particles have a uniform solid spherical morphology with an average size of  $\sim 3.5\text{ }\mu\text{m}$ . After doping Fe into the carbonate, the particles tend to grow into elliptical shapes which are not standard spheres, with a size ranging from 4 to  $6\text{ }\mu\text{m}$ . As shown in Fig. S3(b), the surface of the as-prepared  $\text{MnCO}_3$  microspheres is composed of triangular edges and corners. It seems like that in the solution the crystals are in a radially growing method to form  $\text{MnCO}_3$ . As for the high-magnification image of  $\text{Fe}_{0.2}\text{Mn}_{0.8}\text{CO}_3$  in Fig. S3(d), it looks different with that of

Download English Version:

<https://daneshyari.com/en/article/4756257>

Download Persian Version:

<https://daneshyari.com/article/4756257>

[Daneshyari.com](https://daneshyari.com)